Algebraic chemical shift image reconstruction

Florian Wiesinger[1], Jonathan I Sperl[1], Markus Durst[2], Axel Haase[2], Markus Schwaiger[2], and Rolf F Schulte[3]
[1]GE Global Research, Munich, Germany, [2]Technische Universitaet Muenchen, Munich, Germany, [3]GE Global Research, Germany

Introduction: Metabolic MR imaging using hyperpolarized 13C requires fast chemical shift image (CSI) encoding and reconstruction. Recently, methods based on spiral CSI (1), EPSI (2), and Dixon/IDEAL-type echo shifting (3, 4) have been demonstrated to efficiently address this challenge. These methods require a specific CSI reconstruction and are typically based on simplifying assumptions. In this work a simple and general algebraic CSI reconstruction framework is presented based on a discretized forward model of the encoding process.

Theory and Methods: Chemical shift image encoding is based on repeatedly sampling k-space in different CS phase evolution states. This can be modeled in form of a linear system matrix E, describing the CSI encoding from a priory unknown metabolite images to the actually measured data according to:

$$data_{(p,q)} = E_{(p,q),(m,n)} * image_{(m,n)}\ ,\ with\ E_{(p,q),(m,n)} = e^{ik_p r_n} * e^{i\omega_m t_{p,q}} \quad [1]$$

with $t_{p,q}$ the q^{th} sampling time point of k space location k_p, ω_m the chemical shift frequency, r_n the spatial position vector, and the indices m and n listing metabolites and location, respectively. Chemical shift image decoding/reconstruction can be understood as the inverse problem described by Eq. [1], which for over-determined systems, can be solved in a least-squares sense using the Moore-Penrose-Inverse (†):

$$image_{(m,n)} = E^{\dagger}_{(p,q),(m,n)} * data_{(p,q)} \quad [2]$$

For a typical CSI experiments with e.g. 5 metabolites, image matrix = 32x32pts and 4-fold over-determined data sampling this results in an encoding matrix of dimension 5120x20480 (i.e. 420MB using single precision formation), which can readily be processed and inverted using modern computers.

The CSI encoding described in Eq. [1] can be further refined to additionally account for effects, such as parallel imaging with coil sensitivities $s_u(r_n)$, spatially varying magnetic field inhomogeneity induced off-resonance ($\Delta\omega_{0,n}$), and apparent transverse relaxation effects ($T^*_{2,n}$):

$$\tilde{E}_{(p,q,u),(m,n)} = E_{(p,q),(m,n)} * s_{u,n} * e^{(i\Delta\omega_{0,n} - 1/T^*_{2,n})t_{p,q}} \quad [3]$$

Undesired noise enhancement due to non-ideal conditioning of the encoding matrix can be controlled via truncated singular values decomposition (SVD) based matrix inversion. More specifically, a cut-off threshold (svd_{cut}) can be estimated from the SVD spectrum, corresponding to an effective condition number $\kappa = \max(svd)/svd_{cut}$. In analogy to the g-factor known from parallel imaging (5), an effective number-of-signal average (NSA) metric (4) can be derived to quantify the CS image encoding efficiency according to:

$$NSA_{m,n} = 1/(\boldsymbol{E}^H\boldsymbol{E})^{-1}_{(m,n),(m,n)} \quad [4]$$

Algebraic CSI reconstruction was implemented in R2010b Matlab (MathWorks, Natick, MA) running on a 2.9GHz quad-core CPU with 48GB RAM. Hyperpolarized 13C imaging experiments have been performed on a 3T GE HDx scanner (GE Healthcare, Waukesha, MI) using the HyperSense DNP polarizer (Oxford Instruments, Oxford, UK).

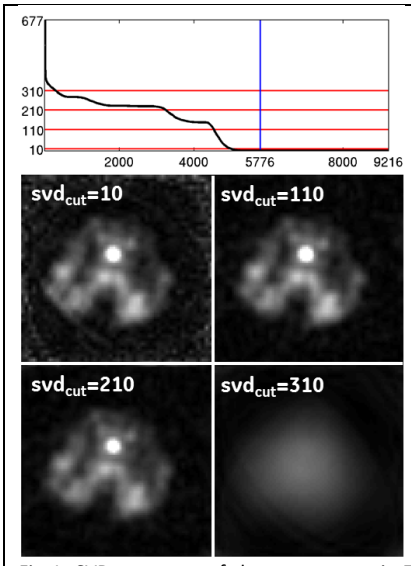

Fig 1: SVD spectrum of the system matrix E and pyruvate metabolite maps for different SVD truncation thresholds (svd_{cut}).

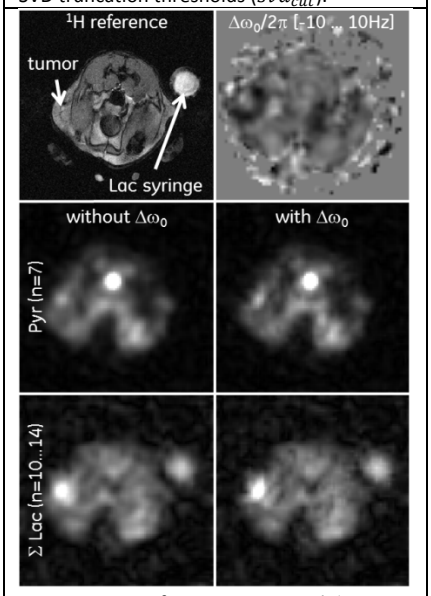

Fig 2: Proton reference image and $\Delta\omega_0$ map (top row). Single time point (n=7) pyruvate (middle row) and time averaged (n=10…14) lactate (bottom row) images without (left) and with (right) off-resonance correction.

Results: In-vivo animal rat experiments were performed with subcutaneously implanted hepatocellular (HCC) tumor. IDEAL spiral CSI images were acquired using 1 FID acquisition and 7 echo-shifted single-shot spirals (ΔTE=1.12ms, FA=5deg, TR=250ms, FOV=8cm, encoding matrix=38x38pts, G_{max}=22mT/m, S_{max}=73T/m/s). 32 time-resolved, single-slice CSI data were encoded at a time resolution of 2s. Figure 1 illustrates the SVD spectrum of the corresponding system matrix according to Eq. [1] for 4 metabolites (pyruvate, pyruvate-hydrate, lactate and alanine) and reconstruction matrix = 48x48pts. The SVD spectrum approaches zero at around the encoding number of 4*38*38=5776 (vertical blue line). The reconstructed pyruvate images illustrate the tradeoff between image noise and resolution mediated by svd_{cut}. Figure 2 shows pyruvate and lactate metabolite maps reconstructed from the same dataset with and without $\Delta\omega_0$ off-resonance correction according to Eq. [3]. $\Delta\omega_0$ was obtained from the minimum-norm, full-spectrum CSI estimation (3) via pixel-wise calculation of the 13C pyruvate center frequency. Off-resonance correction indicates improved spatial resolution with a more localized distribution of the metabolite signals. Initialization, truncated SVD-based matrix inversion, and CSI reconstruction for 32 time steps was finished in ~5mins.

Discussion: The presented method addresses the problem of CSI image reconstruction from the perspective of solving the inverse problem described by the discretized, linear forward encoding model [1]. For typical over-determined systems, the Moore-Penrose-Inverse [2] describes the linear-least square solution, which can be computed via direct truncated SVD-based matrix inversion. The noise/resolution tradeoff can be flexibly adjusted by changing the cut-off threshold in the truncated SVD matrix inversion. With modern numerical computing environments the system matrix E can be setup in a few lines and efficiently be inverted using available SVD-based algorithms (e.g. $pinv(E, svd_{cut})$ in Matlab). All relevant encoding effects can be accounted for in the linear system matrix E, including spectral-spatial gradient encoding, coil sensitivity encoding for parallel imaging, as well as spatially-varying B0 and R2* relaxivity information [3]. The method is not iterative and shortcuts gridding interpolation and density compensation which are otherwise required for non-Cartesian image acquisition.

References: (1) D Mayer et al, MRM 56: 932-7. (2) CH Cunningham et al, JMR 187: 357-62. (3) F Wiesinger et al, MRM: in press. (4) SB Reeder et al, JMRI 26: 1145-52. (5) Pruessmann et al, NMR Biomed 19: 288-99. **Acknowledgements:** This work was co-funded by BMBF MOBITUM grant number 01EZ0826/7 and 01EZ1114.